Slope of the astrophysical S factor for the ^{7}Li$(p,\gamma)^8$Be reaction

M. Spraker,[1,2] R. M. Prior,[1,2] M. A. Godwin,[2,3] B. J. Rice,[2,3] E. A. Wulf,[2,3] J. H. Kelley,[2,3] D. R. Tilley,[2,4] and H. R. Weller[2,3]

[1]*Department of Physics, North Georgia College and State University, Dahlonega, Georgia 30597*

[2]*Triangle Universities Nuclear Laboratory, Duke Station, Durham, North Carolina 27708*

[3]*Department of Physics, Duke University, Durham, North Carolina 27707*

[4]*Department of Physics, North Carolina State University, Raleigh, North Carolina 27695*

(Received 25 January 1999; revised manuscript received 26 July 1999; published 17 December 1999)

Polarized proton beams of 80 and 60 keV, and a biased target have been used to determine the slope of the astrophysical S factor for the ^{7}Li$(p,\gamma)^8$Be reaction from direct measurements at proton energies from 40 to 100 keV for capture to both the ground and the first excited states of ^{8}Be. The results indicate a *negative* slope for both cases. Vector analyzing power measurements at 90° were also obtained for proton energies from 40 to 80 keV. It is shown that the negative slope can be accounted for by considering the effect of the subthreshold resonance state at 16.6 MeV if the capture into this weakly bound, subthreshold state occurs at an effective radius of about 46 fm. The effect of this state increases the extrapolated value of the S factor at $E_p=0$ from the previous value of 0.3 keV b to the present value of 0.50 keV b.

PACS number(s): 25.40.Lw, 27.20.+n, 24.70.+s

I. INTRODUCTION

The radiative capture group at the Triangle Universities Nuclear Laboratory (TUNL) has been engaged in a long term study of low-energy, radiative capture reactions on light nuclei. The current work discusses the latest study of the ^{7}Li$(p,\gamma)^8$Be reaction below 100 keV. Although this reaction is not known to have any major astrophysical importance, this study demonstrates the subtleties involved in extrapolating capture reactions to astrophysical energies even when data exist at very low energies.

The ^{7}Li$(p,\gamma)^8$Be reaction was previously studied below 80 keV using a polarized beam [1]. The results exhibited a large (0.4) analyzing power at $\theta_{\rm Lab}=90°$, indicating the presence of a non-negligible p-wave strength at these extremely low energies. The astrophysical S factor of the ^{7}Li$(p,\gamma)^8$Be reaction was later accurately measured between 100 and 1500 keV [2]. Several efforts were made to explain these data sets by assuming that the $M1$ strength arises from the tails of the 1^+ resonances at 441 and 1030 keV. All of these calculations have been unable to explain the large analyzing power observed at 80 keV, especially when cross section data are also considered [3,4]. Since the amount of p-wave strength in this energy region can play a significant role in extrapolating the S factor to $E=0$, it is important to attempt to understand its physical origin.

Traditional calculations of the ^{7}Li$(p,\gamma)^8$Be reaction at energies below a few hundred keV have assumed pure s-wave $E1$ direct capture. In this model the analyzing power is identically zero. Adding the resonances mentioned above brings in p-wave strength which can generate nonzero analyzing powers. However, detailed calculations have not been able to give a quantitative account of the observed cross section and analyzing powers [3–6]. For example, direct capture-plus-resonance calculations could not produce enough p-wave strength without assigning signs to the various interfering amplitudes which contradicted both shell-model calculations and fits to higher-energy data [5]. This problem was finally overcome [6], or so it seemed, by replacing the direct capture description of the $E1$ strength used in this model by two 1^- resonances, having somewhat adjustable parameters and performing a pure R-matrix calculation, which also included the two $M1$ resonances. This calculation succeeded in producing the larger analyzing power as observed while simultaneously avoiding the problems with the signs of the interfering amplitudes referred to above. However, it also predicted an absolute cross section below 200 keV which is almost a factor of 2 smaller than that measured in Ref. [2], but in agreement with that of Ref. [7].

In the present work it will be shown that a direct measurement of the slope of the S factor for the ^{7}Li$(p,\gamma)^8$Be reaction provides a new observable and new insight into the physics in this energy regime. Previous calculations had produced values for the slope and could therefore be distinguished by a comparison with a measured value. For example, direct-capture-plus-resonances model calculations [3,4] lead to a slope which is close to zero while the pure R-matrix calculation of Ref. [6] mentioned above predicts a rather large positive slope. The results of the present work indicate that the slope is actually *negative* in contradiction with the results of these previous calculations. It will be shown that the effect of the subthreshold state at 16.6 MeV at positive energies is probably the dominant cause of this negative slope. The impact of this on the extrapolation of the S factor to $E=0$ will be discussed.

II. EXPERIMENTAL METHOD

Previous studies at TUNL of the ^{7}Li$(p,\gamma)^8$Be reaction were performed by stopping an 80-keV polarized proton beam in thick evaporated ^{7}Li targets. These targets were fabricated in an evaporator facility, then transferred under argon gas into the scattering chamber. While efforts to avoid oxidation were taken, the present work eliminated this con-

TABLE I. Energy-dependent data taking time periods during a typical target voltage cycle.

Energy (keV)	Data taking time (s)
100	30
95	40
90	60
85	100
80	140
75	180
70	220
65	260
60	300

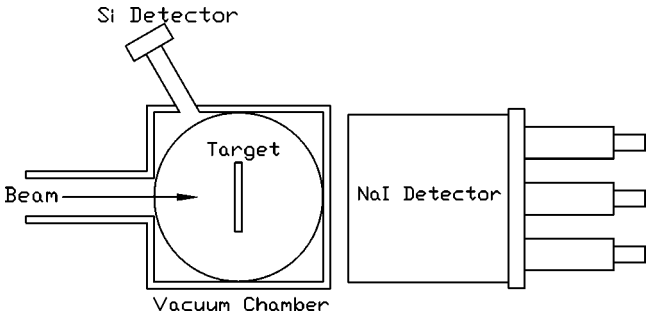

FIG. 1. A sketch of the experimental setup showing the mounting flange for the Si detector and a NaI detector at 0°. The circle represents the location of the 90° NaI detectors. (Not to scale.)

cern by using an *in situ* evaporator, thereby eliminating the tricky transfer process.

The γ rays in the previous works [1,3,4] were detected with both NaI and high-purity germanium (HPGe) detectors. Since the goal of the present experiment was to obtain a direct and accurate measurement of the slope of the *S* factor for this reaction, measurements were needed at energies lower than those previously attempted. While deconvoluting the high-resolution HPGe spectrum is an attractive option, counting rates below $E_p = 80$ keV indicated that the efficiency of these detectors made this an impractical choice. For this reason three 25 cm$\times$25 cm NaI detectors were used, and the beam energy was varied in small steps by biasing the target. This method takes advantage of the high efficiency (total response is about 98% efficient) of the NaI detectors while simultaneously giving incident beam energies in 5-keV increments. With a 25 μA 80 keV beam, the target bias was varied from $+20$ kV to -20 kV in 5 kV steps, which allowed spectra to be obtained at beam energies from 60 to 100 keV. All beams were stopped in the target. The use of two programmable high-voltage power supplies (one for positive and one for negative high voltages) permitted control of the time spent at each energy, as well as the total cycle time. Individual times were adjusted to compensate for the rapidly decreasing count rate and provide similar statistical accuracy at each setting. A typical cycle lasted less than 1 h, with each energy receiving times as shown in Table I. Relatively short cycle times allowed many cycles to be run during the course of the experiment (about six 24-h days), thus greatly reducing systematic uncertainties between the data obtained at different energies.

One disadvantage of this technique is that it makes reliable charge integration difficult, if not impossible. However, this disadvantage is offset by running with a very stable beam current and cycling through all energies frequently, thereby canceling the effects of any long term drifts in beam current on the relative yields. The time spent at each energy is a relative measure of the total number of incident projectiles at each energy. While this alone could leave some uncertainty, the rather prolific α particle yield from the ^{7}Li$(p,\alpha)^4$He reaction which has been previously measured as a function of energy in this regime was used to test the present technique by a direct comparison with prior results.

There were two significant controls which were used to validate the accuracy of these data. First, the experiment was repeated with a 60-keV beam. Although previous tests using beam viewers had indicated that there were no observable effects on the beam spot size or distribution as a result of the target bias, the 60-keV measurements allowed testing of this observation since there were data between 60 and 80 keV obtained both by biasing the target negatively (thereby increasing the beam energy from 60 up to 80 keV) and by biasing it positively (thereby decreasing the beam energy on target from the incident 80 keV down to 60 keV). Both measurements gave the same slope in this energy region of overlap, providing strong evidence that target biasing was not adversely affecting the measured values of the slope. These measurements with a 60-keV beam also provided very important new data between 40 and 60 keV. In this case, due to the very reduced count rates below 60 keV, the step size used on the bias voltage was changed from 5 to 10 kV.

The second important control was the simultaneous measurement of the ^{7}Li$(p,\alpha)^4$He reaction. These measurements were performed using a 500 μm thick silicon surface-barrier detector set at a scattering angle of 135°. This detector was contained in a tube which extended it beyond the ground plane of the scattering chamber, as shown in Fig. 1. Besides providing geometrical convenience, this arrangement and a 0.1 mil Ni foil which covered the front face of the detector eliminated background effects due to low-energy scattered protons and secondary electrons. Care was taken to be sure that the silicon detector was collimated so that it saw the full target area. Since the count rate in this detector was about 100 times as great as the γ-ray channel, good statistics were obtained. More importantly, this higher count rate made it much easier to obtain reliable energy-dependent data for this channel versus the γ ray channels, even when doing one energy at a time. Previous workers have obtained rather consistent data for the slope of the *S* factor in the ^{7}Li$(p,\alpha)^4$He reaction. It was a requirement that the present experiment reproduce these values.

The three 25 cm$\times$25 cm NaI detectors used to detect the γ rays going to the ground ($E_\gamma = 17.3$ MeV) and first excited states ($E_\gamma = 14.3$ MeV) of ^{8}Be were placed so that two were at 90° on opposite sides of the beam line, and one was at 0°. In addition, one of the 90° detectors was surrounded by a plastic anticoincidence shield which was used to reject cosmic rays. The rejection efficiency achieved during this ex-

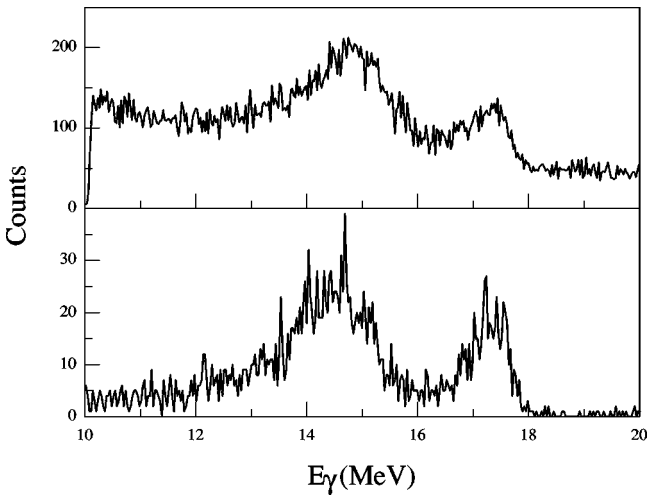

FIG. 2. Raw spectra for the $^{7}\mathrm{Li}(p,\gamma)^{8}\mathrm{Be}$ reaction both with (below) and without (above) the active scintillating shield.

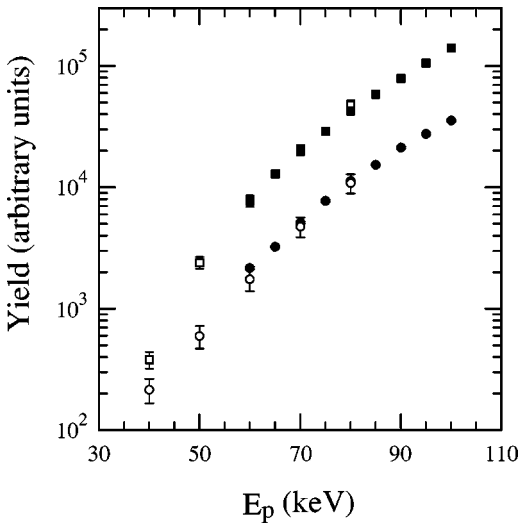

FIG. 3. The $^{7}\mathrm{Li}(p,\gamma_0)^{8}\mathrm{Be}$ (circular points) and $^{7}\mathrm{Li}(p,\gamma_1)^{8}\mathrm{Be}$ (square points) yields at 90° from 40 to 100 keV. The open points are data from the 60 keV data set, and the solid points were taken from the 80 keV set. The yields at each energy have been normalized to correspond to the same data taking time. The error bars indicate the statistical uncertainties of the data points. When not shown, the uncertainty is smaller than the size of the data point.

periment was 98.5%. While the rejected spectra were easier to analyze and made background subtraction unambiguous, the results obtained with the unshielded NaI detectors were in excellent agreement with those obtained with the shielded detector.

III. DATA ANALYSIS

A. Extracting yields from spectra

The first step in processing these data was to extract sums from the raw spectra. Typical spectra from the unshielded and the shielded NaI detectors are shown in Fig. 2. A relative yield was obtained by summing from one half-width above to two half-widths below the centroid of each peak. Cosmic ray background was subtracted from the region of interest by summing events above the region of interest and normalizing this sum to the number of channels in the region of interest before subtracting it.

Since the data were taken under similar beam and target conditions for all energies, the various yields could be compared once they were normalized to the same data taking time. The results for the gamma-ray data from both 90° detectors combined are shown in Fig. 3 for capture to the ground and to the first excited state of $^{8}\mathrm{Be}$. The figure contains the data from both the 60-keV and the 80-keV beam runs, normalized in the region of overlap. It is important to note that the energy dependence in this region agrees for the two runs, as desired.

B. Obtaining the slope of the *S* factor

The goal was to extract the slope of the astrophysical *S* factor from these data. This *S* factor is defined in terms of the cross section according to

$$\sigma(E_{\mathrm{c.m.}})=\frac{S(E_{\mathrm{c.m.}})}{E_{\mathrm{c.m.}}}e^{-31.29Z_1Z_2\sqrt{\mu}/\sqrt{E_{\mathrm{c.m.}}}}, \tag{1}$$

where Z_1 and Z_2 are the charges of the projectile and target, μ is the reduced mass in amu, and $E_{\mathrm{c.m.}}$ is in keV. At the low energies of this experiment $S(E)$ was assumed to be a linear function of energy:

$$S(E_{\mathrm{c.m.}})=S_0+S_1{*}E_{\mathrm{c.m.}}. \tag{2}$$

The validity of this assumption was tested by the ability to fit the measured data with it.

The measured yield was an integrated yield from the beam energy to zero energy (the beam stopped in the thick target) at each beam energy. In order to determine S_0 and S_1 from the data, an iterative calculation of the yield was made. At each incident beam energy, the target was divided into a series of 1 $\mu\mathrm{g/cm}^2$ layers. The yield was calculated for the first layer, using assumed values of the *S*-factor parameters to calculate the cross section at that energy. The energy loss of the beam in that layer was calculated and the yield calculation was repeated for the next layer at the decreased energy. This proceeded until the yield was negligible for successive layers. The total yield was the sum of the yields for each of the layers. The energy losses for protons in lithium were taken from Anderson and Ziegler [8]. This procedure was done at each beam energy and applied iteratively, adjusting the *S*-factor parameters until a fit to the data was obtained.

C. The analyzing power data

A 25-μA polarized proton beam, obtained from the TUNL atomic beam polarized ion source, was used to obtain all of the present data. The beam polarization was measured using the spin-filter [9] technique, and was typically found to be 0.60 ± 0.03. The direction of the spin of the incident beam was reversed at the rate of 10 Hz, and data were sorted into spin-up and spin-down spectra. These spectra were then used

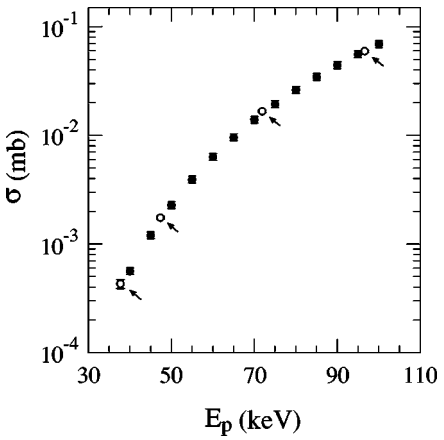

FIG. 4. The ^{7}Li(p,α) reaction yield normalized to the cross section data reported by Rolfs and Kavanagh [10]. The arrows indicate the data from Ref. [10]. The error bars indicate the statistical uncertainties of the data points.

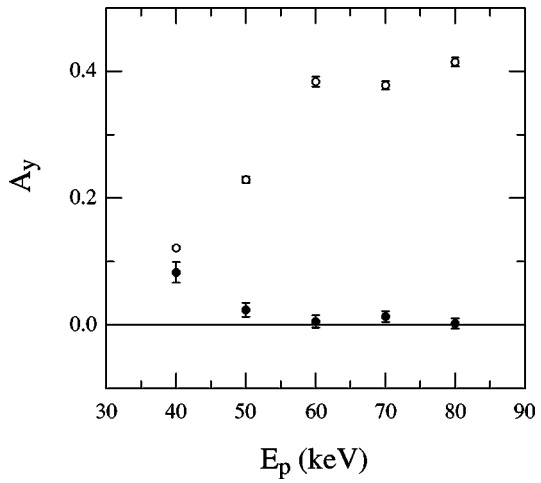

FIG. 5. The vector analyzing power at 90° for the ^{7}Li$(p,\gamma_0)^8$Be (open points) and ^{7}Li$(p,\gamma_1)^8$Be (solid points) reactions. The error bars indicate the statistical uncertainties of the data points.

to extract a spin-up and a spin-down yield at each beam energy using the previously described procedure. The results were then combined to calculate the analyzing power, $A_y(90°)$, at each energy according to

$$A_y(90°)=\frac{Y^u(90°)-Y^d(90°)}{(p^d)Y^u(90°)+(p^u)Y^d(90°)}, \tag{3}$$

where Y^u and Y^d are the spin-up and spin-down yields and $p^{u,d}$ are the polarizations of the spin-up and spin-down beams, respectively.

IV. EXPERIMENTAL RESULTS

A. ^{7}Li$(p,\alpha)^4$He cross section data

The data obtained for the ^{7}Li$(p,\alpha)^4$He reaction at $\theta=135°$ are shown in Fig. 4. The data obtained with the 60 and 80 keV beams were normalized in the region of overlap. Note that the energy dependence exhibited by both data sets is identical to within statistical uncertainty. The absolute scale shown here was obtained by normalizing the present results to those of [10]. The data from [10] are also shown in Fig. 4 for comparison, and it is seen that the agreement is excellent.

The data of Fig. 4 for the present experiment were used to obtain values for S_0 and S_1, defined in Eq. (2), by fitting the data using the previously described iterative process. The values obtained were $S_0=49\pm4.4$ keV b, and $S_1=0.036\pm0.003$ b. These results are in excellent agreement with the previous results reported in [10].

This result provides significant evidence that the present method of measuring the energy dependence of the cross section and of extracting the slope of the *S* factor from the data is sound. It is also important to note that the slope of the *S* factor obtained from these high-statistics data is not negative, indicating that there is not a systematic problem in this technique which produces negative slopes.

B. The ^{7}Li$(p,\gamma_{0,1})^8$Be cross section data

The time normalized yields, obtained as described in Sec. III A, are shown for capture to the ground and first-excited states in Fig. 3. These data were fitted in order to determine the values of S_0 and S_1. The absolute normalization of the cross section was obtained by normalizing the present data to that of [2] at 98.3 keV. The results for the case of capture to the ground state (γ_0) were $S_0=0.50\pm0.07$ keV b and $S_1=(-9.5\pm3.2)\times10^{-4}$ b. A negative slope was also obtained for the case of capture to the first excited state (γ_1), where $S_0=1.86\pm0.25$ keV b and $S_1=(-2.5\pm0.5)\times10^{-3}$ b.

The analyzing power data obtained for capture to the ground and first excited states at 90° are shown in Fig. 5. Data are available only from 40 to 80 keV because the beam polarization was unstable for the 60 to 100 keV data set. The results at 80 keV are in good agreement with previous results [1,3,4] obtained by stopping an 80 keV beam in a ^{7}Li target. The present results indicate that the analyzing power for capture to the ground state decreases from 0.4 to about 0.25 as the energy decreases from 80 to 40 keV. The analyzing power results for γ_1 are consistent with zero [as are the 0° results for both cases, as they must be (not shown)].

V. INTERPRETATION AND CALCULATION

A. Implications of the negative slope

The slope of the *S* factors for the reactions ^{12}C$(\alpha,\gamma)^{16}$O, ^{7}Be$(p,\gamma)^8$B, and ^{16}O$(p,\gamma_{0,1})^{17}$F have been the subject of several recent papers [11–15]. In the case of ^{12}C$(\alpha,\gamma)^{16}$O, the unknown relative phase between the 1^- subthreshold resonance and the lowest-lying above threshold 1^- resonance drastically affects the extrapolated values of the *S* factor [11]. Negative slopes are predicted by direct capture calculations for both the ^{7}Be$(p,\gamma)^8$B and the ^{16}O$(p,\gamma_1)^{17}$F reactions. As pointed out in [13], since capture in both of these reactions is external, the *S* factors at the relevant energies are determined by the product of the spectroscopic factor, the asymptotic normalization of the final-state wave

functions, and a pure Coulomb term. In both reactions, the weakly bound final state is responsible for the rise in the S factor as the center-of-mass energy approaches 0. This rise has been shown to be due to a pole at $E_\gamma = 0$ induced by the weakly bound final states which are, in fact, halo in nature.

It seems extremely unlikely that a similar effect is responsible for the negative slope which is observed in the present case of $^7\mathrm{Li}(p,\gamma)^8\mathrm{Be}$ capture to the ground state since the proton single-particle ground state of ^{8}Be is tightly bound by over 17 MeV. Indeed, pure $E1$ direct capture calculations predict a slope which is essentially zero below 100 keV, with small differences in the various calculations arising from the different choices of potentials used to describe the scattering state [2,4,5]. When the two $M1$ resonances at 441 and 1030 keV are added to this direct strength, as in Ref. 4, the slope becomes positive. This was also found to be the case in a pure R-matrix calculation of the reaction [6] which included the same two $M1$ resonances as above but used two 1^- resonances in place of a direct $E1$ capture amplitude. In fact, a microscopic cluster model calculation of this reaction [17] predicts a slope which is, although very slightly negative, almost zero and quite like that obtained from direct-capture-plus-resonances model calculations [2].

B. Calculating the negative slope

To explain the negative slope, the effect of the bound 2^+ state of ^{8}Be at 16.6 MeV was considered. The influence of this state has not been included in previous work. This almost totally isospin mixed ''protonlike'' state is only bound by about 630 keV (versus 17 MeV for the ground state) and its $T=1$ component is the analog of the (halo) ground state of ^{8}B [16]. In the capture to the ground state, this state would enter as a subthreshold resonance.

An attempt to include this state in a direct-capture-plus-resonances model calculation, where it is populated by p-wave capture followed by $E2$ decay to the ground state, indicated that it had little or no effect for any reasonable resonance parameters. However, its extended halolike nature can be observed when one performs a direct p-wave $E2$ capture calculation of the $^7\mathrm{Li}(p,\gamma)^8\mathrm{Be}$ reaction leading to this state. In this calculation the (final) state was represented as a p-wave single-particle state, generated using a Woods-Saxon potential which reproduced the experimentally known binding energy (630 keV). A plot of the direct capture integrand is shown in Fig. 6. This result is very similar to that of Fig. 4 in [15], which showed a plot for the p-wave ($E1$) direct capture integrand leading to the halo $\frac{1}{2}^+$ state of ^{17}F.

This observation led to a new calculation. Instead of simply adding the resonance amplitude to the $E1$ direct capture amplitude, a form factor was inserted in the numerator of the resonance amplitude which allowed control of the region of space where the resonance contribution was located. The formalism for this is based on the direct semidirect model [18], which combines the direct amplitude and the resonance (semidirect) amplitude radial terms as

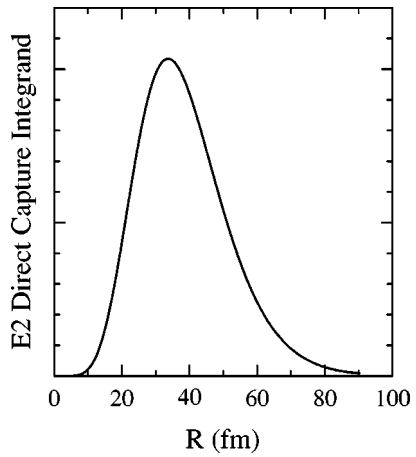

FIG. 6. The integrand of the $E2$ direct-capture matrix element leading to the 16.6 MeV state plotted as a function of the radius.

$$\langle u(r)|r|\chi^+(r)\rangle + \langle u(r)|\frac{h(r)}{E-E_R+i\frac{\Gamma}{2}}|\chi^+(r)\rangle, \qquad (4)$$

Direct amplitude+resonance amplitude with $h(r)$ included,

where $\chi^+(r)$ is the incident wave function and $u(r)$ is the wave function of the bound final state. The functional form of $h(r)$ was that of a derivative Woods-Saxon potential [19]. The parameters were adjusted to reproduce the radial dependence observed in Fig. 6 as well as possible. The resonance parameters of the 16.6 MeV state were based on previously determined values [20] and were

$$E_x = 16.626 \text{ MeV}$$
$$(\text{corresponding to } E_R = -0.628 \text{ MeV}),$$
$$\Gamma_{\text{tot}} = 130 \text{ keV}.$$

The strength of $h(r)$ was adjusted to provide the best fit to the data. The deduced strength is consistent with the experimental value of Γ_γ (70 ± 25 meV) [20] assuming a spectroscopic factor of 1.0. A calculation was performed which in-

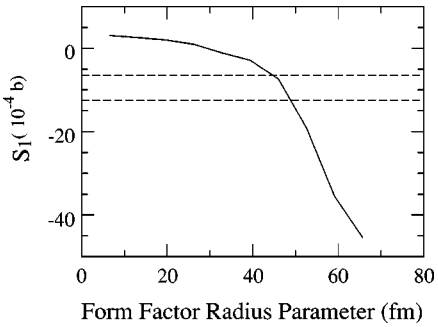

FIG. 7. The slope (solid line) of the calculated S factor (S_1) for the $^7\mathrm{Li}(p,\gamma_0)^8\mathrm{Be}$ reaction as a function of the radius at which the direct-capture integrand peaks for the 16.6-MeV 2^+ subthreshold resonance in ^{8}Be. The dotted lines show the range of values allowed by experiment.

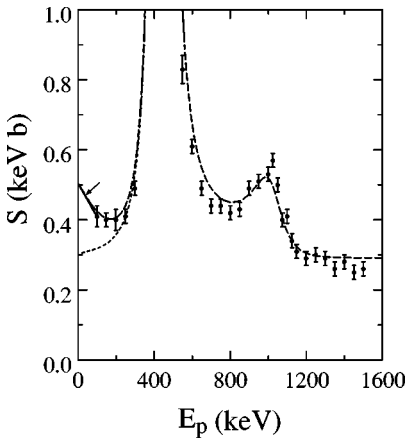

FIG. 8. Calculations showing the effect of the 16.6-MeV 2^+ subthreshold resonance in ^{8}Be on the low-energy behavior of the S factor for the $^7\mathrm{Li}(p,\gamma_0)^8\mathrm{Be}$ reaction. The short dashed curve below 400 keV shows the calculation containing direct capture and the two higher $M1$ resonances. The long dashed curve includes the 16.6-MeV subthreshold state in addition. The data shown in this figure are from Zahnow *et al.* [2]. The line segment between 0 and 100 keV, indicated by the arrow, is the deduced result from the present measurement.

cluded the direct $E1$ amplitude and the 16.6 MeV 2^+ subthreshold resonance only. The radius parameter of the form factor $h(r)$ was varied and the slope of the S factor was computed as a function of this radius. The results are shown in Fig. 7 along with the experimentally determined value of the slope. Figure 7 shows that the effective radius at which this subthreshold resonance is formed is 46 ± 3 fm. When the cross section is calculated with this resonance included using this effective radius, the results obtained are as shown in Fig. 8. As shown here, the weakly bound subthreshold state can play a significant role in determining the behavior of the cross section at near-threshold energies. In this case, it is responsible for an increase in the S factor at $E=0$ from the previously deduced value of about 0.3 keV b to the present value of about 0.5 keV b.

Although the slope and cross section of the present experimental data below $E_p=100$ keV are well accounted for by this direct capture plus subthreshold resonance calculation, a full calculation which includes the higher lying $M1$ resonances as well as other effects such as the coupling to other channels is needed. Attempts to describe all of the observables (including the angular distributions of cross sections and analyzing powers) of this and previous work using a direct-capture-plus-resonances model has not been successful. There are a considerable number of free resonance and potential parameters, including phases, which make such calculations somewhat arbitrary. A more complete microscopic model calculation is needed. However, the results of these limited calculations point out the important role played by the weakly bound states when they are properly included. These states should be included in any future works.

The results indicate that negative slopes of S factors can arise not only in the case when one is capturing to a weakly bound halolike state, but also in the case of capture to tightly bound states if a weakly bound subthreshold state is present, as in the case of $^7\mathrm{Li}(p,\gamma)^8\mathrm{Be}$.

VI. CONCLUSIONS

A new method has been employed to directly measure the low-energy slope for the astrophysical S factor of the $^7\mathrm{Li}(p,\gamma)^8\mathrm{Be}$ reaction. It uses a computer-controlled power supply to bias the target in steps allowing for measurement of the integrated yield at several different incident energies around a single beam energy. Due to the rapidity of the stepping procedure data at very different energies can be taken under the same beam and target conditions.

The study of the $^7\mathrm{Li}(p,\gamma)^8\mathrm{Be}$ reaction has shown that at low energies, previously made assumptions about the relative simplicity of radiative capture reactions are unfounded. The results discussed in this paper indicate that the slope of the astrophysical S factor can be strongly affected by both subthreshold and positive energy resonances in the residual nucleus. Future extrapolations of the S factor to astrophysically relevant energies should take this into account.

[1] R. M. Chasteler, H. R. Weller, D. R. Tilley, and R. M. Prior, Phys. Rev. Lett. **72**, 3949 (1994).
[2] D. Zahnow, C. Angulo, C. Rolfs, S. Schmidt, W. H. Schulte, and E. Somorjai, Z. Phys. A **351**, 229 (1995).
[3] M. A. Godwin, R. M. Chasteler, C. M. Laymon, R. M. Prior, D. R. Tilley, and H. R. Weller, Phys. Rev. C **53**, R1 (1996).
[4] M. A. Godwin, C. M. Laymon, R. M. Prior, D. R. Tilley, and H. R. Weller, Phys. Rev. C **56**, 1605 (1997).
[5] F. C. Barker, Aust. J. Phys. **48**, 813 (1995).
[6] F. C. Barker, Aust. J. Phys. **49**, 1081 (1996).
[7] F. E. Cecil, D. Ferg, H. Liu, J. C. Scorby, J. A. McNeil, and P. D. Kunz, Nucl. Phys. **A539**, 75 (1992).
[8] H. H. Anderson and J. F. Ziegler, *Hydrogen Stopping Powers and Ranges in all Elements* (Pergamon, New York, 1977).
[9] A. J. Mendez, C. D. Roper, J. D. Dunham, and T. B. Clegg, Rev. Sci. Instrum. **67**, 3073 (1996).
[10] C. Rolfs and R. W. Kavanagh, Nucl. Phys. **A455**, 179 (1986).
[11] G. Wallerstein *et al.*, Rev. Mod. Phys. **69**, 995 (1997).
[12] K. Riisager and A. S. Jensen, Phys. Lett. B **301**, 6 (1993).
[13] B. K. Jennings, S. Karataglidis, and T. D. Shoppa, Phys. Rev. C **58**, 579 (1998).
[14] W. Schwab *et al.*, Z. Phys. A **350**, 283 (1995).
[15] R. Morlock, R. Kunz, A. Mayer, M. Jaeger, A. Muller, J. W. Hammer, P. Mohr, H. Oberhummer, G. Staudt, and V. Kolle, Phys. Rev. Lett. **79**, 3837 (1997).
[16] T. Minamisono *et al.*, Phys. Rev. Lett. **69**, 2058 (1992).
[17] A. Csoto and S. Karataglidis, Nucl. Phys. **A607**, 62 (1996).
[18] H. R. Weller and N. R. Roberson, Rev. Mod. Phys. **52**, 699 (1980).
[19] M. C. Wright, H. Kitazawa, N. R. Roberson, H. R. Weller, M. Jensen, and D. R. Tilley, Phys. Rev. C **31**, 1125 (1985).
[20] L.-De Braeckeleer *et al.*, Phys. Rev. C **51**, 2778 (1995).